Toxicology and Applied Pharmacology 268 (2013) 331–342

Contents lists available at SciVerse ScienceDirect

Toxicology and Applied Pharmacology

journal homepage: www.elsevier.com/locate/ytaap

Action of hexachlorobenzene on tumor growth and metastasis in different experimental models

Carolina Andrea Pontillo [a], Paola Rojas [b], Florencia Chiappini [a], Gonzalo Sequeira [b], Claudia Cocca [c], Máximo Crocci [d], Lucas Colombo [e], Claudia Lanari [b], Diana Kleiman de Pisarev [a], Andrea Randi [a,*]

[a] Laboratorio de Efectos Biológicos de Contaminantes Ambientales, Departamento de Bioquímica Humana, Facultad de Medicina, Universidad de Buenos Aires, Buenos Aires, Argentina
[b] Laboratorio de Carcinogénesis Hormonal, Instituto de Biología y Medicina Experimental (IBYME-CONICET), Buenos Aires, Argentina
[c] Laboratorio de Radioisótopos, Facultad de Farmacia y Bioquímica, Universidad de Buenos Aires, Buenos Aires, Argentina
[d] Instituto de Inmunooncología Crescenti, Buenos Aires, Argentina
[e] Instituto de Oncología Angel Roffo, Universidad de Buenos Aires, Buenos Aires, Argentina

ARTICLE INFO

Article history:
Received 17 October 2012
Revised 13 February 2013
Accepted 14 February 2013
Available online 24 February 2013

Keywords:
Hexachlorobenzene
MDA-MB-231
Cell invasion
AhR
MMPs
Metastasis

ABSTRACT

Hexachlorobenzene (HCB) is a widespread organochlorine pesticide, considered a possible human carcinogen. It is a dioxin-like compound and a weak ligand of the aryl hydrocarbon receptor (AhR). We have found that HCB activates c-Src/HER1/STAT5b and HER1/ERK1/2 signaling pathways and cell migration, in an AhR-dependent manner in MDA-MB-231 breast cancer cells. The aim of this study was to investigate *in vitro* the effect of HCB (0.005, 0.05, 0.5, 5 μM) on cell invasion and metalloproteases (MMPs) 2 and 9 activation in MDA-MB-231 cells. Furthermore, we examined *in vivo* the effect of HCB (0.3, 3, 30 mg/kg b.w.) on tumor growth, MMP2 and MMP9 expression, and metastasis using MDA-MB-231 xenografts and two syngeneic mouse breast cancer models (spontaneous metastasis using C4-HI and lung experimental metastasis using LM3). Our results show that HCB (5 μM) enhances MMP2 expression, as well as cell invasion, through AhR, c-Src/HER1 pathway and MMPs. Moreover, HCB increases MMP9 expression, secretion and activity through a HER1 and AhR-dependent mechanism, in MDA-MB-231 cells. HCB (0.3 and 3 mg/kg b.w.) enhances subcutaneous tumor growth in MDA-MB-231 and C4-HI *in vivo* models. *In vivo*, using MDA-MB-231 model, the pesticide (0.3, 3 and 30 mg/kg b.w.) activated c-Src, HER1, STAT5b, and ERK1/2 signaling pathways and increased MMP2 and MMP9 protein levels. Furthermore, we observed that HCB stimulated lung metastasis regardless the tumor hormone-receptor status. Our findings suggest that HCB may be a risk factor for human breast cancer progression.

Introduction

Hexachlorobenzene (HCB) is an environmental pollutant which was used as a fungicide, and it is still released into the environment as a byproduct in several industrial processes. Chronic exposure of laboratory animals to HCB elicits a number of effects such as thyroid dysfunctions (Alvarez et al., 2005), porphyria (Mylchreest and Charbonneau, 1997) and promotion of rat mammary tumors (Randi et al., 2006). The International Agency for Research on Cancer classifies HCB as a probable human carcinogen (Agency for Toxic Substances, Disease Registry, ATSDR, 2002).

HCB is a dioxin-like compound and a weak ligand of the aryl hydrocarbon receptor (AhR) (Hahn et al., 1989), which is a ligand-dependent transcription factor that modulates processes such as apoptosis, proliferation and migration (Dietrich and Kaina, 2010). Upon dioxin binding, AhR can translocate to the nucleus where it regulates gene transcription (Matsumura, 1994). On the other hand, AhR-dioxin may release c-Src from its cytosolic complex, which can stimulate growth factor receptors, including the human epidermal growth factor receptor (HER1) (Park et al., 2007).

Breast cancer is the most common type of cancer diagnosed in the developing world and most of their deaths are due to metastases (Wang et al., 2007). Matrix metalloproteases (MMPs) are a family endoproteinases that are involved in the degradation of the extracellular matrix (ECM), and contribute to cancer initiation or growth as well as cell invasion and metastasis (Duffy et al., 2000). The gelatinases A (MMP2) and B (MMP9) are associated with increased malignancy of tumor cells, because of their unique ability to degrade the type-IV colagen of the basement membrane (Chambers and Matrisian, 1997).

Tumorigenesis frequently occurs as a result of the overexpression of proteins that are otherwise involved in normal cellular processes,

* Corresponding author at: Laboratorio de Efectos Biológicos de Contaminantes Ambientales, Departamento de Bioquímica Humana, Facultad de Medicina, Universidad de Buenos Aires, Paraguay 2155, 5to piso, (C1121ABG) Buenos Aires, Argentina. Fax: +54 11 4508 3672.
E-mail addresses: caroponti@hotmail.com (C.A. Pontillo), parojas2010@gmail.com (P. Rojas), florenciachiappini@hotmail.com (F. Chiappini), chicon27_7@hotmail.com (G. Sequeira), cm_cocca@hotmail.com (C. Cocca), info@crescenti.com.ar (M. Crocci), lucascol2003@yahoo.com.ar (L. Colombo), lanari.claudia@gmail.com (C. Lanari), dianakleiman@yahoo.com.ar (D. Kleiman de Pisarev), andybiol@yahoo.cm.ar (A. Randi).

0041-008X/$ – see front matter © 2013 Elsevier Inc. All rights reserved.
http://dx.doi.org/10.1016/j.taap.2013.02.007

like HER1 and c-Src (Biscardi et al., 1999a). HER1 and c-Src co-overexpression and association leads to the c-Src-mediated phosphorylation of tyrosine 845 (Y-845) of the HER1 (Biscardi et al., 1999b), and results in EGF-induced phosphorylation of the signal transducers and activators of transcription 5b (STAT5b) on Y-699 (Kloth et al., 2003). Furthermore, HER1 can stimulate the mitogen-activated protein kinases pathway (ERK1/2) (Parsons and Parsons, 2004). These pathways are involved in cell growth, apoptosis, invasion, and migration (Wang et al., 2007).

In our previous work, we found that HCB activated AhR, c-Src/HER1/STAT5b and HER1/ERK1/2 signaling pathways, in the estrogen receptor α (ERα) negative MDA-MB-231 breast cancer cell line (Pontillo et al., 2011). Herein, we examined the ability of HCB to promote cell invasion, MMP2 and MMP9 expression, secretion and activation, and whether the AhR and c-Src/HER1 signaling pathways are involved in HCB-induced effects, in MDA-MB-231. Furthermore, we studied the action of HCB on tumor growth, MMP2 and MMP9 expression and metastasis in MDA-MB-231 orthotopically xenotransplanted female nude mice and in two metastatic syngeneic models: C4-HI a hormone receptor positive cancer model (Lanari et al., 2009) and LM3 a hormone receptor negative tumor model (Urtreger et al., 1997). Finally, using the MDA-MB-231 xenograft model we studied if c-Src/HER1 signaling pathway is involved in HCB-induced effects.

Materials and methods

Chemicals

HCB (>99% purity, commercial grade) was obtained from Aldrich-Chemie GmbH & Co. (Steinheim, Germany). Anti-HER1, anti-c-Src, anti-phospho-Y416-c-Src and anti-phospho-ERK1/2 antibodies were purchased from Cell Signaling Technology, Inc. (MA). Anti-ERK1/2, anti-STAT5b and anti-phospho-Y699-STAT5b antibodies were obtained from Upstate (Lake Placid, NY) and anti-phospho-Y845-HER1 antibody was obtained from Abcam Ltd. (Cambridge, UK). Anti-MMP2 antibody was purchased from Santa Cruz Biotechnology (CA, USA); and anti-MMP9 antibody as well as GM6001, a general MMPs inhibitor, was obtained from Millipore (Temecula, California, USA). Anti-β-Actin, 4,7-orthophenanthroline (4,7 PHE), and α-naphthoflavone (α-NF) were obtained from Sigma Chemical Co. (St. Louis, MO). The enhanced chemiluminescence kit (ECL) was from GE Healthcare Life Sciences (Buckinghamshire, UK). 4-Amino-5-(4-chloro-phenyl)-7-(t-butyl) pyrazolo[3,4-d]pyrimidine (PP2) inhibitor was obtained from Calbiochem (La Jolla, CA) and tyrphostin AG1478 inhibitor was purchased from A.G. Scientific, Inc. (San Diego, CA). RPMI-1640 culture medium was purchased from HyClone Laboratories, Inc. (Logan, UT). Antibiotic–antimycotic, trypsine, and glutamine were obtained from PAA Laboratories GmbH (Pasching, Austria). The random primers were obtained from Biodynamics, Argentina. Enzymes and cofactors for reverse transcription (RT) and polymerase chain reaction (PCR) were purchased from Promega Corporation (Madison, WI). The kit SYBR Green Supermix (Applied Biosystems) and the specific oligonucleotides for human MMP2 and MMP9 were obtained from Invitrogen Life Technologies (UK). All other reagents used were of analytical grade.

Cell culture and treatment

MDA-MB-231 cell line (American Type Culture Collection) derives from a metastatic site (pleural effusion) of a human breast adenocarcinoma. Cells were cultured at 37 °C in a 5% CO_2 incubator with RPMI-1640 with 10% fetal bovine serum (FBS), 1% antibiotic–antimycotic mixture (10,000 Units/ml penicillin, 10 mg/ml streptomycin sulfate, and 25 μg/ml amphotericin B), and 1% glutamine. After 24 hours of starvation, cells at 70–80% confluence were treated with HCB (0.005, 0.05, 0.5 and 5 μM) dissolved in absolute ethanol. Final ethanol concentration in each treatment was 0.5% and had no influence on the analyzed parameters as shown previously (García et al., 2010). For inhibitors treatment, cells were pretreated for 3 hours with the specific inhibitors, PP2 for c-Src, AG1478 for HER1, and 4,7-orthophenanthroline (4,7 PHE) and α-naphthoflavone (α-NF) for AhR, as well as GM6001 for MMPs. Then, HCB or vehicle was added to the media in the presence or absence of inhibitors, according to the assay. LM3 murine mammary carcinoma cell line (Roffo Oncology Institute, Buenos Aires, Argentina) was culture with MEM media. When LM3 was inoculated into BALB/c tail vein, multiple metastatic foci are visible in the lung 3 weeks later (Urtreger et al., 1997).

Tumors

C4-HI (independent hormone) tumors are ductal murine mammary carcinomas which express high ER and progesterone receptors (PR) levels. These tumors have metastatic capacity in axilar lymphatic node and lung, and are antiprogestin, tamoxifen and antiestrogen responsive (Lanari et al., 2009).

Animals and treatment

Six- to eight-week-old female nude Swiss mice and female BALB/c mice (La Plata Laboratory Animal Facility, Buenos Aires, Argentina) were maintained in a controlled environment: 24 ± 2 °C, 50 ± 10% relative humidity, and a 12–12 hours light/dark cycle. Female nude mice were housed into germ free environmental conditions. HCB (0.3, 3 and 30 mg/kg body weight) was dissolved in corn oil and then administered by intraperitoneal injection (i.p.) (0.1 ml) three times a week. Control animals were injected i.p. with corn oil (0.1 ml) as a vehicle. All the procedures were conducted in accordance with the Guide for the Care and Use of Laboratory Animals, National Research Council, USA. This research project was evaluated and accepted by the Institutional Animal Care and Use Committee (CICUAL) of School of Medicine, University of Buenos Aires, Argentina (Res.1146/2011).

Metastasis breast cancer models

a) MDA-MB-231 xenograft model in nude Swiss mice. MDA-MB-231 cells (6×10^6) were injected into the mammary fat pad of nude mice. When tumors reached a volume of 50 mm^3, animals were treated with HCB or vehicle for 30 days. Tumors were measured three times a week and the volume of the tumors were calculated (πLW2/6; L: length, W: width). At the time of necropsy, tumors were excised, weighed, measured, photographed and then one portion was fixed for histological analysis, and the other one was used for Western blot. Lungs, livers and lymph nodes were embedded in paraffin, sectioned, stained with hematoxylin–eosin (HE) and the presence of micrometastasis in these organs was evaluated in seriates slices.

b) C4-HI syngeneic model in BALB/c mice. C4-HI tumors were orthotopic transplanted in female BALB/c mice. All procedures were similar as described for the MDA-MB-231 xenograft model.

c) LM3 syngeneic model in BALB/c mice. BALB/c mice were treated with HCB or vehicle during 2 weeks. After that, LM3 (5×10^4) cells were injected into the tail vein of mice and then, animal treatment was continued for another 3 weeks. Animals were euthanized and lungs were fixed in Bouin. Finally, the number and size (mm) of metastatic foci per lung were evaluated under stereoscopic microscope. Results were expressed as number of total metastatic foci per lung, and as number of metastatic foci with diameters smaller or larger than 1.5 mm.

Gelatin zymography

Aliquots (25–50 μl) of cell-conditioned media were resuspended in Laemmli modified buffer [10 mM Tris–HCl (pH 6.8), 2% sodium

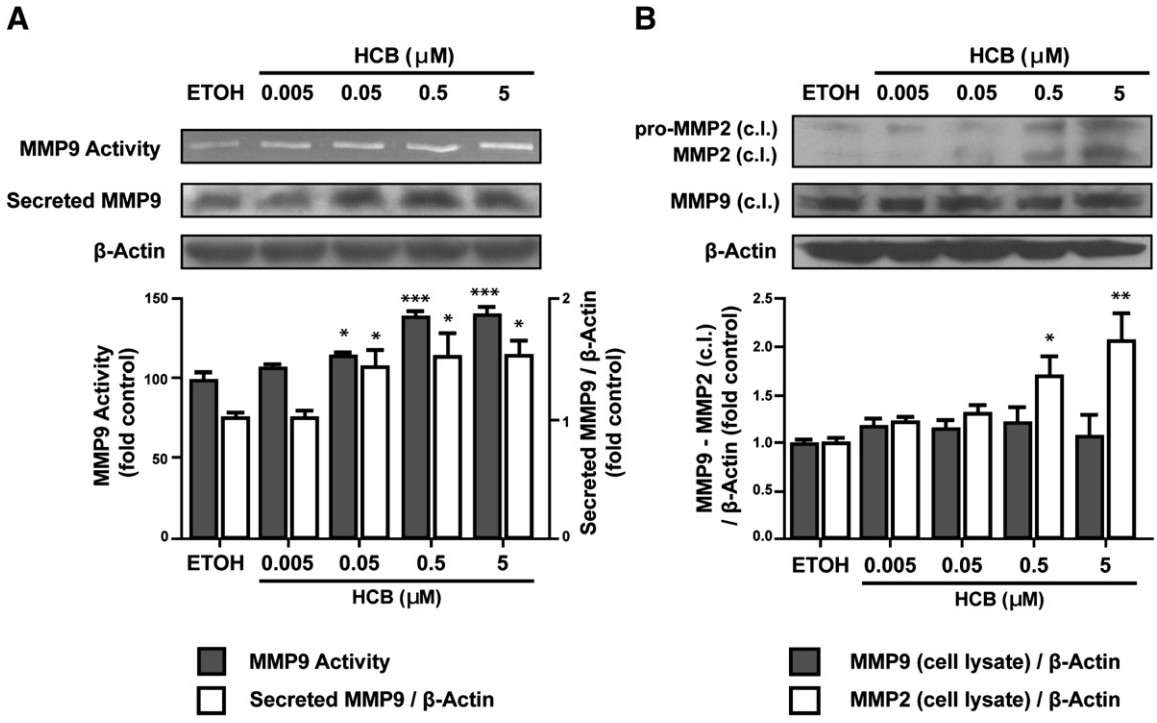

Fig. 1. Dose–response of HCB effect on MMPs expression, secretion and activity. (A) MMP9 activity and protein level secreted; (B) intracellular MMP2 and MMP9 protein levels in MDA-MB-231. Cells were treated with HCB (0.005, 0.05, 0.5, and 5 μM) or vehicle during 24 h. Cell-conditioned media were collected and whole-cell lysates were prepared. (A) MDA-MB-231-conditioned media was collected and MMP9 activity quantified by gelatin zymography, and protein levels were analyzed by Western blot. (B) Whole-cell lysates were used to measure intracellular MMP2 and MMP9 protein levels by Western blot. Intracellular or secreted protein MMPs levels, and activity were relativized to β-Actin expression. One representative experiment is shown in the upper panels. Quantification by densitometric scanning of the immunoblots or MMP activity is shown in the lower panels. Data are expressed as means ± SDs of three independent experiments. Asterisks indicate significant differences vs. control ($^{*}p < 0.05$, $^{**}p < 0.01$, $^{***}p < 0.001$), ANOVA and Tukey post hoc test.

dodecyl sulfate (SDS), 0.03% bromophenol blue, 10% glycerol], and denatured at 95 °C for 5 min. Samples were loaded on 6 or 7.5% SDS–PAGE gels containing 1% gelatin and electrophoresed. After electrophoresis, gels were washed twice with Rinsing I buffer [50 mM Tris–HCl (pH 7.4), 2.5% Triton X-100], for 30 min, and then three times with Rinsing II buffer [50 mM Tris–HCl (pH 7.4)], for 5 min, to remove SDS, and subsequently incubated during 24, 48 or 72 h at 37 °C in developing buffer containing [50 mM Tris–HCl, 0.15 M NaCl and 10 mM CaCl2 (pH 7.4)]. Metalloprotease activity was visualized, by 0.5% Coomassie brilliant blue R-250 staining. Gels were scanned and clear bands were quantified by scanning laser densitometry in a Fotodyne (Foto/Analyst), Gel-Pro Analyzer 3.1. Values were normalized by immunoblotting using anti-β-Actin antibody. Each experiment was repeated at least three times, and the results were normalized to arbitrary units, designating a value of 100 to control assays.

Preparation of nuclear protein extracts and subcellular fractionation

Mammary tumors of female nude mice were homogenized in 0.2 M sucrose, 10 mM Hepes, 15 mM KCl, 2 mM EDTA and 0.5 mM dithiothreitol (pH 7.6) supplemented with protease inhibitors [(2.5 mM benzamidin, 10 μg/ml aprotinin, 1 μg/ml pepstatin A, 1 μg/ml leupeptin, 0.5 mM phenylmethylsulfonyl fluoride (PMSF)] and phosphatase inhibitors (2 mM Na3VO4 and 50 mM NaF) in an Elvejhem-type glass homogenizer, and subcellular fractionation prepared according to Peña et al. (2012). Protein concentration was determined according to Bradford (1976) using bovine serum albumin as standard.

Western blotting

Total cellular protein lysates and subcellular fractions (30–80 μg) were used by Western blot analysis as described Pontillo et al. (2011). Polyclonal anti-phospho-Y845-HER1 (1:250), anti-phospho-Y416-c-Src (1:500), anti-phospho-ERK1/2 (1:1000), anti-phospho-Y699-STAT5b (1:500), anti-HER1 (1:500), anti-c-Src (1:500), anti-ERK1/2 (1:1000), anti-STAT5b (1:500), anti-MMP2 (1:500), anti-MMP9 (1:500) as well as monoclonal anti-β-Actin (1:2000) antibodies were used.

RNA preparation and Real-Time quantitative PCR

MDA-MB-231 was treated with HCB (5 μM) or vehicle during 16 or 24 h. Total RNA was isolated from MDA-MB-231 cells using TRI-reagent/chloroform extraction according to manufacturer's protocol. An aliquot of 1 μg of total RNA was used to synthesize first-strand cDNA. The resulting cDNA product was used as template for quantitative PCR (qPCR) analysis using kit SYBR Green Supermix (Applied Biosystems) and iCycler PCR thermocycler (Bio-Rad). Specific oligonucleotides for human MMP2 (forward: 5′-GAATGCCATCCCCG ATAACC-3′ and reverse: 5′-GGTTCTCCAGCTTCAGGTAATAGG-3′) and MMP9 (forward: 5′-CCTCGCCCTGAACCTGAGC- 3′ and reverse: 5′-GCTCTGAGGGGTGGACAGTG-3′) were utilized. GAPDH expression was used as a control to normalize the data.

Transwell invasion assay

Invasive activity was quantified using a transwell chamber (8 μm pore size) coated with 13% Matrigel (50 μl/well) in RPMI medium and then was incubated during 2 h at 37 °C and 5% CO2 for gelification. Approximately 2.5×10^4 cells per well were seeded onto the Matrigel-coated wells and incubated in serum free medium with HCB (5 μM) or vehicle for 48 h. RPMI with 10% SFB was added to the bottom chamber as chemoattractant. Non invading cells were removed from the upper chamber with a moistened cotton swab. Cells that had migrated through the membrane to the lower surface were fixed with ice-cold methanol, stained with 0.5% toluidine blue, and

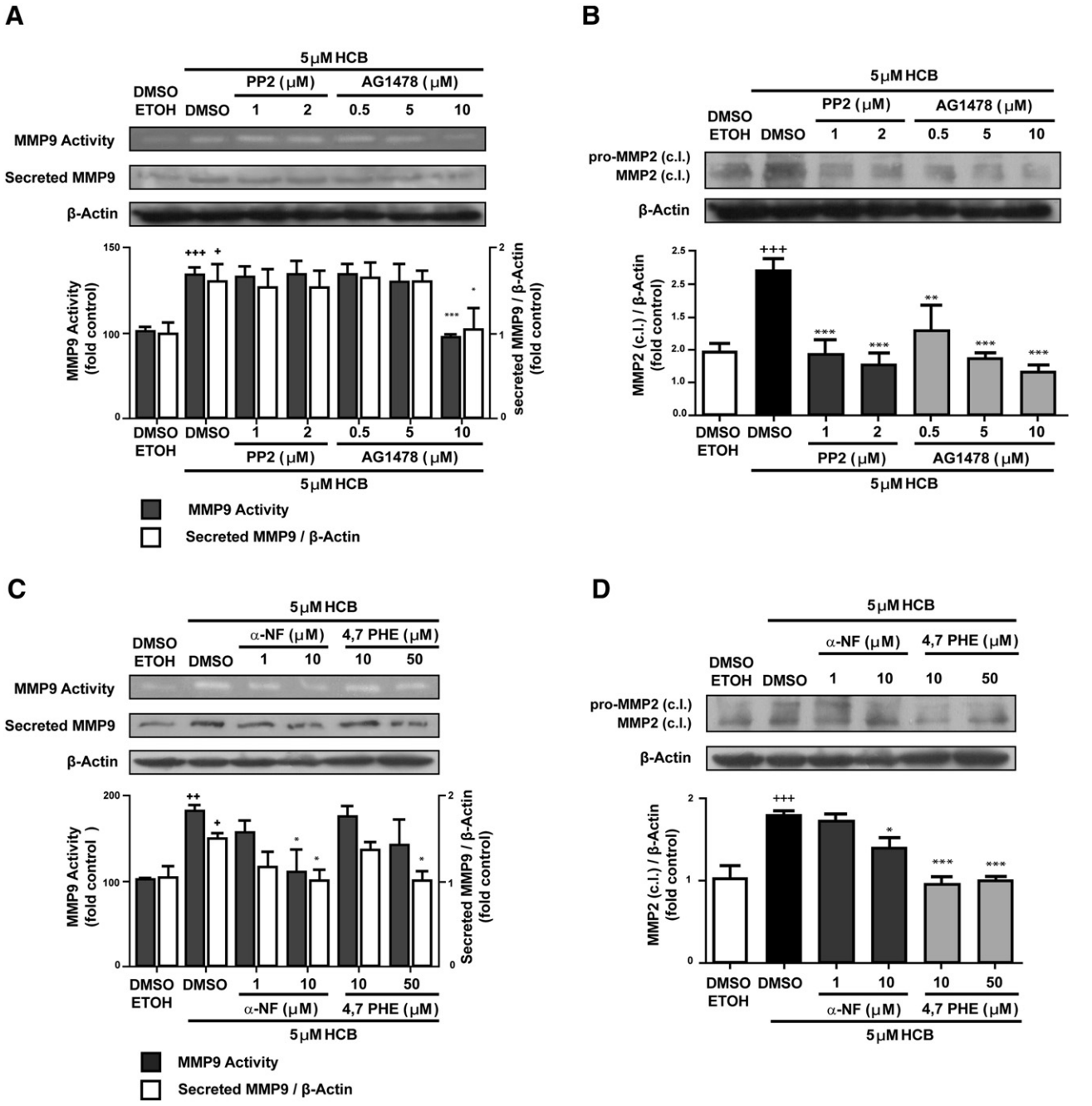

Fig. 2. c-Src, HER1 and AhR roles in HCB-induced changes on MMPs activity and protein levels in MDA-MB-231. (A,C) MMP9 activity and secreted protein levels; (B,D) intracellular MMP2 protein levels. Cells were pretreated with PP2 (1 and 2 μM), AG1478 (0.5, 5 and 10 μM), α-NF (1 and 10 μM) or 4,7 PHE (10 and 50 μM) for 3 h, and then were treated with HCB (5 μM) or vehicle during 24 h in the presence or absence of inhibitors. (A,C) MDA-MB-231-conditioned medium was used to measure MMP9 activity by gelatin zymography and protein levels were analyzed by Western blot. (B,D) Whole-cell lysates were used to measure intracellular MMP2 levels by Western blot. Data were normalized to β-Actin. One representative experiment is shown in the upper panels. Quantification by densitometric scanning of the immunoblots or MMP activity is shown in the lower panels. Data are expressed as means ± SDs of three independent experiments. Asterisks indicate significant differences vs. HCB 5 μM (*$p < 0.05$, **$p < 0.01$ and ***$p < 0.001$). Crosses indicate significant difference versus vehicle (DMSO + ETOH), (+$p < 0.05$, ++$p < 0.01$ and +++$p < 0.001$), ANOVA and Tukey post hoc test.

counted under a light microscope. Each experiment was repeated at least three times, and the results were normalized to arbitrary units, designating a value of 100 to control assays.

Statistical analysis

To compare differences in tumor growth, the tumor volume data were analyzed by two-way ANOVA followed by Bonferroni post hoc test for treatment comparisons. Data from the others assays were evaluated by one-way ANOVA, followed by Tukey post hoc test to identify significant differences between controls and treatments. To compare differences in Q-RT-PCR assay, the mRNA levels data were analyzed by Student's *t*-test. Differences were considered significant when p values were <0.05. Results represent the mean ± SD of at least three independent experiments.

Results

HCB effect on MMPs in MDA-MB-231

Since HCB promotes MDA-MB-231 cell migration (Pontillo et al., 2011), we investigated the pesticide effects on MMP2 and MMP9

expression, secretion and activity in this cell line. HCB (0.05, 0.5 and 5 μM) increased MMP9 secretion (44, 53 and 54%) and activity (16, 40 and 40%, Fig. 1A). MMP2 protein levels in the conditioned media were undetectable, suggesting that MMP2 expression level is lower than that of MMP9 in MDA-MB-231 cells. However, HCB 0.5 and 5 μM significantly increased MMP2 protein levels in cell lysates (70 and 105%) (Fig. 1B).

c-Src, HER1 and AhR roles in HCB-induced changes on MMPs

Recently, we have reported that HCB stimulates c-Src/HER1/STAT5b and HER1/ERK1/2 signaling pathways in MDA-MB-231 (Pontillo et al., 2011). Thus, we hypothesized that c-Src and HER1 may be involved in the HCB-induced regulation of MMPs. Only the HER1 inhibitor (AG1478, 10 μM) abrogated the HCB-induced increase in MMP9 secretion and activity (Fig. 2A). Conversely, both the c-Src (PP2) and HER1 (AG1478) inhibitors, prevented the HCB stimulation of intracellular MMP2 protein levels, at all assayed doses (Fig. 2B). Altogether these results indicate that HER1 is involved in HCB-induced MMP9 expression, secretion and activity, while both c-Src and HER1 are implicated in HCB-increased MMP2 expression.

Recent investigations suggest that AhR participates in MMPs expression and activity regulation (Ishida et al., 2010; Peng et al., 2009). As shown in Fig. 2C, α-NF (10 μM) blocked the increase in HCB-induced MMP9 secretion and activity, while 4,7 PHE (50 μM) only inhibited the increase in MMP9 secretion. Our results also show that both α-NF (10 μM) and 4,7 PHE (10 and 50 μM), inhibited the HCB-induced MMP2 expression (Fig. 2D). These results demonstrate that AhR is involved in HCB-induced MMP9 secretion and activity, and in MMP2 expression.

HCB modifies MMPs mRNA levels

Since MMP2 and MMP9 protein levels are increased by HCB, we evaluated MMPs mRNA levels at different times of HCB (5 μM) exposure in Q-RT-PCR assay. The pesticide significantly increased MMP2 (140 %) and MMP9 (65 %) mRNA levels at 16 h of treatment (Fig. 3A), returning to control values at 24 h (Fig. 3B).

HCB action on cell invasion

We examined next the effect of HCB on MDA-MB-231 invasive capacity. As shown in Fig. 4A cell invasion is significantly enhanced by HCB (245%). Because it is well established that c-Src, HER1 and AhR could be involved in cell invasion (Miller et al., 2005), we next analyzed if these proteins were also involved in HCB-induced effect. Our results indicate that c-Src, HER1 and AhR are implicated in HCB-induced cell invasion (Figs. 4A and B). We also evaluated if HCB-induced increase on cell invasion is mediated by MMPs, using GM6001, a general MMPs inhibitor. Our results show that MMPs are involved in the invasion induced by HCB (5 μM) (Fig. 4A).

Mouse xenograft model

HCB effect on MDA-MB-231 tumors

In an attempt to analyze HCB action *in vivo*, we used an orthotopic mouse xenograft model with MDA-MB-231. Our results showed that HCB (0.3 and 3 mg/kg b.w.) significantly increased tumor volume and weight (Figs. 5A and B). Then, we analyze if HCB modifies c-Src/HER1 pathway in MDA-MB-231 tumors. As shown in Fig. 6A, the pesticide enhanced phospho-Y416-c-Src levels at all assayed doses, whereas total c-Src levels were not changed. Moreover, treatment of mice with HCB (3 and 30 mg/kg b.w.) increased Y845-HER1 phosphorylation, as well as total HER1 levels at all assayed doses (Fig. 6B). These results suggest that treatment of mice with HCB (0.3, 3 and 30 mg/kg b.w.) stimulates Y416-c-Src and Y845-HER1 phosphorylation in MDA-MB-231 xenotransplanted mammary tumors.

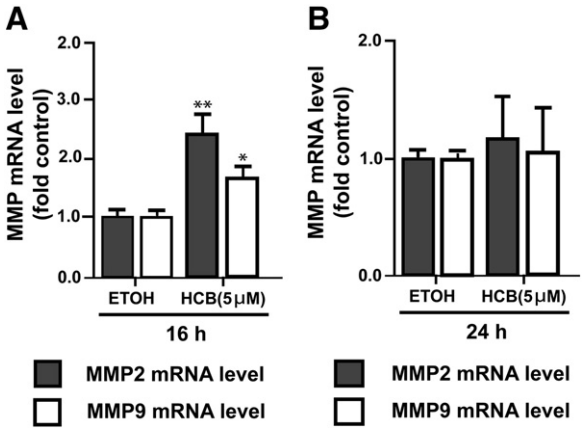

Fig. 3. Enhancement of MMPs mRNA levels in MDA-MB-231 by HCB-treatment. (A) HCB effects on MMPs mRNA levels at 16 h, and (B) at 24 h. MDA-MB-231 was exposed to HCB (5 μM) or vehicle during 16 or 24 h. Total RNA was purified and analyzed for mRNA expression by Q-RT-PCR using the oligonucleotides indicated in Materials and methods. GAPDH expression was used as a control to normalize the data. The values are mean ± SD of three independent experiments. Asterisks indicate significant differences vs. control (*$p < 0.05$, **$p < 0.01$) analyzed by Student's *t*-test.

In order to evaluate HCB action on STAT5b and ERK1/2 phosphorylation, cytosolic and nuclear fractions of tumors were electrophoresed and immunoblotted. Furthermore, we found that in HCB-treated mice, the pesticide significantly increased nuclear total and phospho-ERK1/2 levels at all assayed doses (Fig. 6C). HCB (3 and 30 mg/kg b.w.) enhanced cytosolic Y699-STAT5b phosphorylation, while nuclear total and phospho-Y699-STAT5b levels were increased at all assayed doses (Fig. 6D). Our results clearly indicate that HCB enhances ERK1/2 and STAT5b activation and translocation to the nucleus in MDA-MB-231 xenotransplanted mammary tumors (Figs. 6C and D).

Given the promoting role of MMPs in tumor initiation and progression, we have investigated if HCB-induced mammary tumor growth correlates with an increase in MMPs levels in these tumors. Since MMPs are proteolytic enzymes that must be secreted to extracellular media, we considered to study MMPs levels in microsomal fractions of mammary tumors which contain secretory vesicles. As shown in Figs. 6E and F, HCB increased MMP2 and MMP9 protein levels at all assayed doses, indicating that the pesticide could be stimulating MMPs expression in tumors.

HCB action on metastasis in MDA-MB-231 xenograft model

The current study demonstrated that the pesticide enhances MDA-MB-231 cell invasion. As the *in vivo* xenograft model reproduces mostly all of HCB effects observed with MDA-MB-231 cell line *in vitro*, we examined whether HCB could modify the ability of this cell line to metastasize to lung, liver and lymph node. As metastasis in these tissues were registered in few control and treated mice, we could not arrive to any significant conclusion. However, it is important to highlight that 1 or 2 out of 10 mice developed lung metastasis among the HCB-treated mice, meanwhile no mice in the vehicle control group developed lung metastasis (data not shown). To better understand HCB action on metastasis, we continue studying the pesticide effect on two others animal metastasis syngeneic models into BALB/c mice: a spontaneous model, C4-HI mammary carcinomas transplanted s.c. and an experimental model, LM3 cells inoculated i.v.

Mouse syngeneic spontaneous metastasis model

In order to evaluate HCB effects in C4-HI mammary carcinomas transplanted s.c. into female BALB/c mice, we analyzed first whether the pesticide alters tumor growth. Similarly to the outcomes acquired

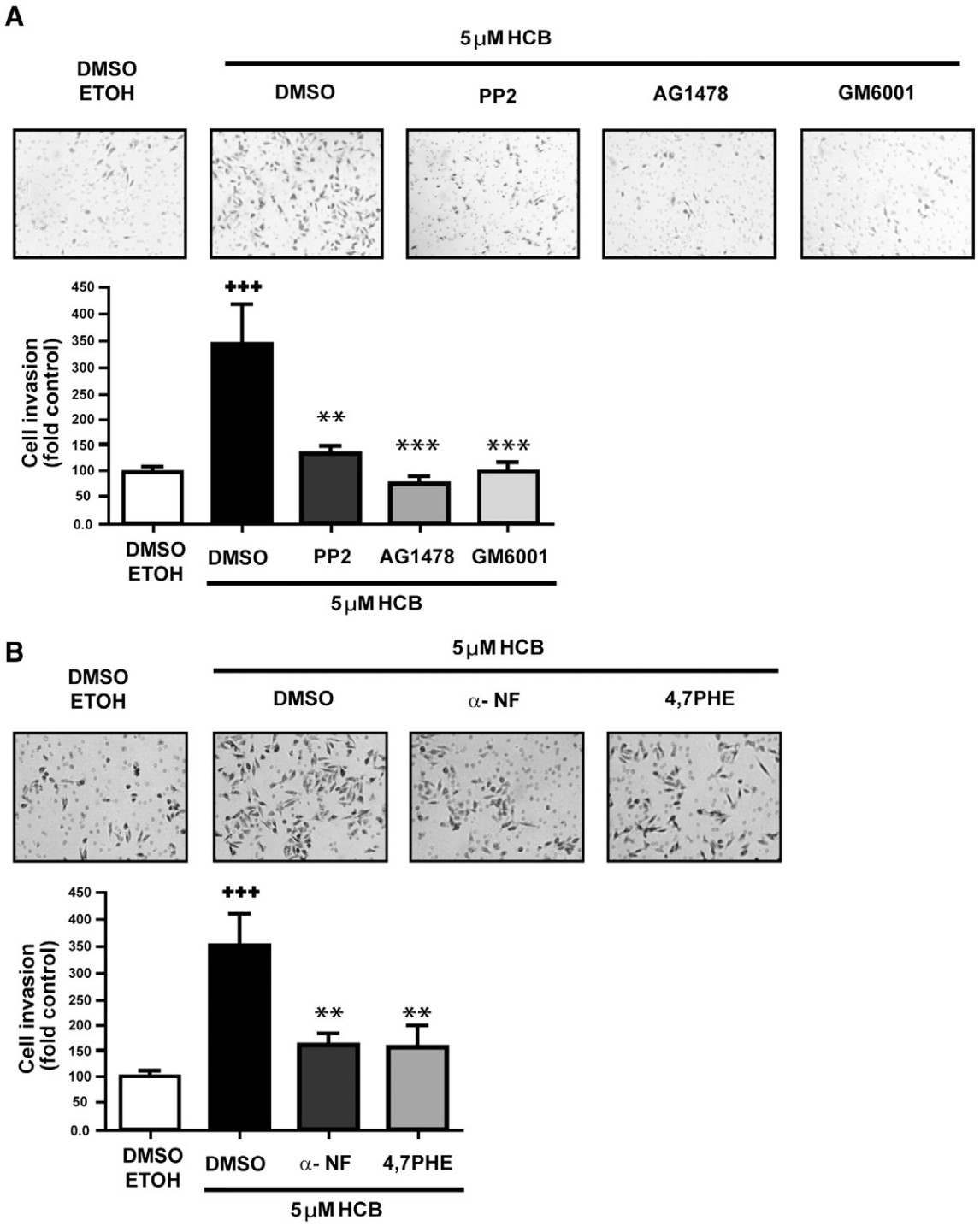

Fig. 4. HCB action on cell invasion. Roles of c-Src, HER1, AhR and MMPs. Effect of HCB on cell invasion and studies with (A) PP2, AG1478 or GM6001 inhibitors; and (B) 4,7 PHE or α-NF inhibitors. Cells were pretreated for 3 h with specific inhibitors (2 μM PP2, 10 μM AG1478, 10 μM GM6001, and 10 μM 4,7 PHE or α-NF). Then, 2.5×10^4 cells were suspended in serum free media with HCB (5 μM) in the presence or absence of inhibitors and placed on the top of transwell chambers covered with matrigel. RPMI with 10% FBS was placed in the lower chamber as chemoattractant. After incubation for 48 h, the cells on the lower surface of the filters were fixed, stained, and counted under an optic microscope. The number of cells that had invaded through the filter was counted and represented as mean ± SD. Crosses indicate significant differences versus vehicle (DMSO + ETOH) ($+++p < 0.001$). Asterisks indicate significant differences versus 5 μM HCB ($^{**}p < 0.01$, $^{***}p < 0.001$), ANOVA and Tukey post hoc test.

with the mouse xenograft model, we observed that HCB (0.3 and 3 mg/kg b.w.) significantly enhanced C4-HI tumor volume and tumor weight (Figs. 7A and B). We also evaluated if HCB could modify the capability of C4-HI tumors to metastasize to lungs, livers and lymph nodes in BALB/c mice. The presence of micrometastasis in stained sections of paraffin-embedded lungs, livers and lymph nodes were analyzed. Our results show that all mice developed lung and liver metastasis. Conversely, no mice developed lymph node metastasis in either of these groups (data not shown). Representative photomicrographs of histological sections of normal lung and liver, as well as lung and liver micrometastasis from vehicle and HCB-treated mice are shown in Fig. 8A. Since this model presented higher levels of metastasis than the xenograft model, a statistical analysis of the number of lung or liver micrometastasis for each group was made. HCB-treated mice (0.3 and 3 mg/kg b.w.) significantly increased the number of lung micrometastasis (Fig. 8B), while only the lowest

A

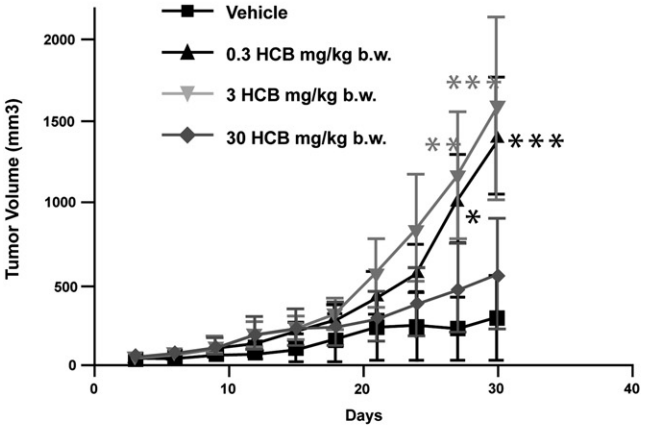

B

	Vehicle	0.3 HCB mg/kg bw	3 HCB mg/kg bw	30 HCB mg/kg bw
Tumor weight (g)	0.10 ± 0,05	1.33 ± 0,3 *	1.33 ± 0,6 *	0.13 ± 0,6

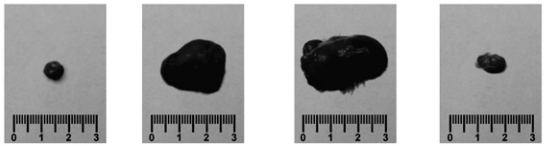

C

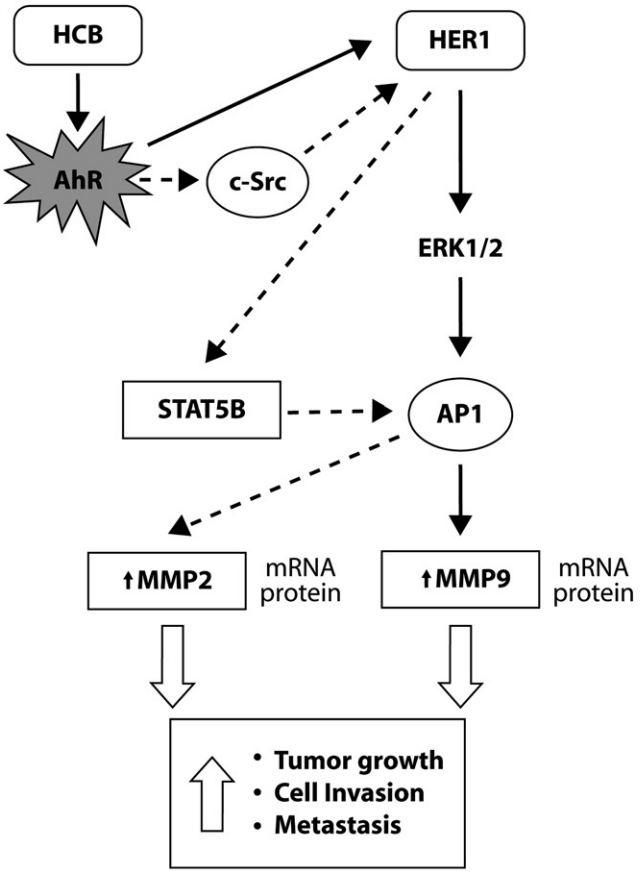

Fig. 5. HCB enhances mammary tumor growth in a mouse xenograft assay. (A) Tumor volume and (B) tumor weight. (C) The overall scheme for HCB-induced effects on MMPs, cell invasion and tumor growth. MDA-MB-231 cells (6×10^6) were injected into the mammary fat pad of mice as described in Materials and methods. Once tumors reached a volume of 50 mm^3, HCB (0.3, 3, 30 mg/kg b.w.) or vehicle was administered i.p., and tumors were measured three times a week. Animals were euthanized at 30 days after treatment and then tumors were photographed, weighed and measured. (A) Tumor volume (mm^3) versus time (days). Statistical comparisons were made by analysis of variance (two-way ANOVA) with a 95% confidence. ANOVA: interaction, treatment factor and time factor $p < 0.0001$. ANOVA analysis was followed by Bonferroni for treatment comparisons. The values are mean ± SD of three experiments with $n = 10$ mice per group. Asterisks indicate significant differences versus vehicle ($^*p < 0.05$, $^{**}p < 0.01$, $^{***}p < 0.001$). (B) The values are mean ± SD of three independent experiments with $n = 10$ mice per group. Asterisks indicate significant differences vs. vehicle ($^*p < 0.05$), ANOVA and Tukey post hoc test.

HCB dose enhanced the number of liver micrometastasis (Fig. 8C). These results indicated that HCB treatment of BALB/c mice enhances the capability of C4-HI mammary tumors to metastasize to lung and liver, according to the assayed doses.

Mouse syngeneic experimental lung metastasis LM3 model

To evaluate if HCB promotes metastasis in the LM3 model, mice were treated i.p. with HCB (0.3, 3 and 30 mg/kg b.w.) during 2 weeks, and then LM3 cells were injected into the tail vein of mice, and HCB-treatment was continued for another 3 weeks. Our results showed that HCB does not change the number of total metastatic foci in lungs (Fig. 9A); however the pesticide significantly enhanced the number of metastatic foci with diameter larger than 1.5 mm in HCB (30 mg/kg b.w.) treated mice (Fig. 9D).

Discussion

Investigation of environmental contributions to breast cancer risk may provide opportunities for prevention of the most common cancer among women. The hypothesis that organochlorine compounds increase the risk of breast cancer in humans is based on the carcinogenicity and hormone-like effects of many organochlorines (Connor et al., 1997).

Previously, we have shown that HCB stimulates c-Src/HER1/STAT5b and HER1/ERK1/2 signaling pathways in MDA-MB-231 cells, *in vitro* (Pontillo et al., 2011). In this study, we have demonstrated that HCB 5 μM stimulates MMP9 expression, secretion and activity via HER1/ERK1/2 pathway in this cell line. Thus, a possibility in our investigation is that ERK1/2 triggers MMP9 gene transcription via AP-1 as reported by other authors (Luo et al., 2009) (Fig. 5C). On the other hand, we observed that HCB 5 μM induces MMP2 expression by c-Src/HER1/STAT5b pathway. Similarly, other authors have also demonstrated the involvement of c-Src and HER1 pathways in MMP9 and/or MMP2 enhanced expression, secretion and activity (Lee et al., 2007; Soto-Guzmán et al., 2010). MMPs expression has not been directly associated with STAT5b. Nevertheless, Catterall et al. (2001) suggested that activated STAT5b could induce c-Fos expression, triggering an increase of MMP2 protein levels via AP-1 (Fig. 5C).

Recent studies suggest that AhR can modulate MMPs expression and activities, as well as cell motility and invasion (Kung et al., 2009). In this respect, we have previously shown that AhR is involved in HCB-induced migration and signaling pathways activation in MDA-MB-231 (Pontillo et al., 2011). Herein, we found that HCB-induced enhancement of MMP9 secretion and activity as well as MMP2 expression are mediated by AhR in this cell line. In a similar manner, Meng et al. (2009) observed that benzopirene-induced MMPs expression is AhR-dependent. Villano et al. (2006) found that AhR is involved in TCDD increased MMP2 and

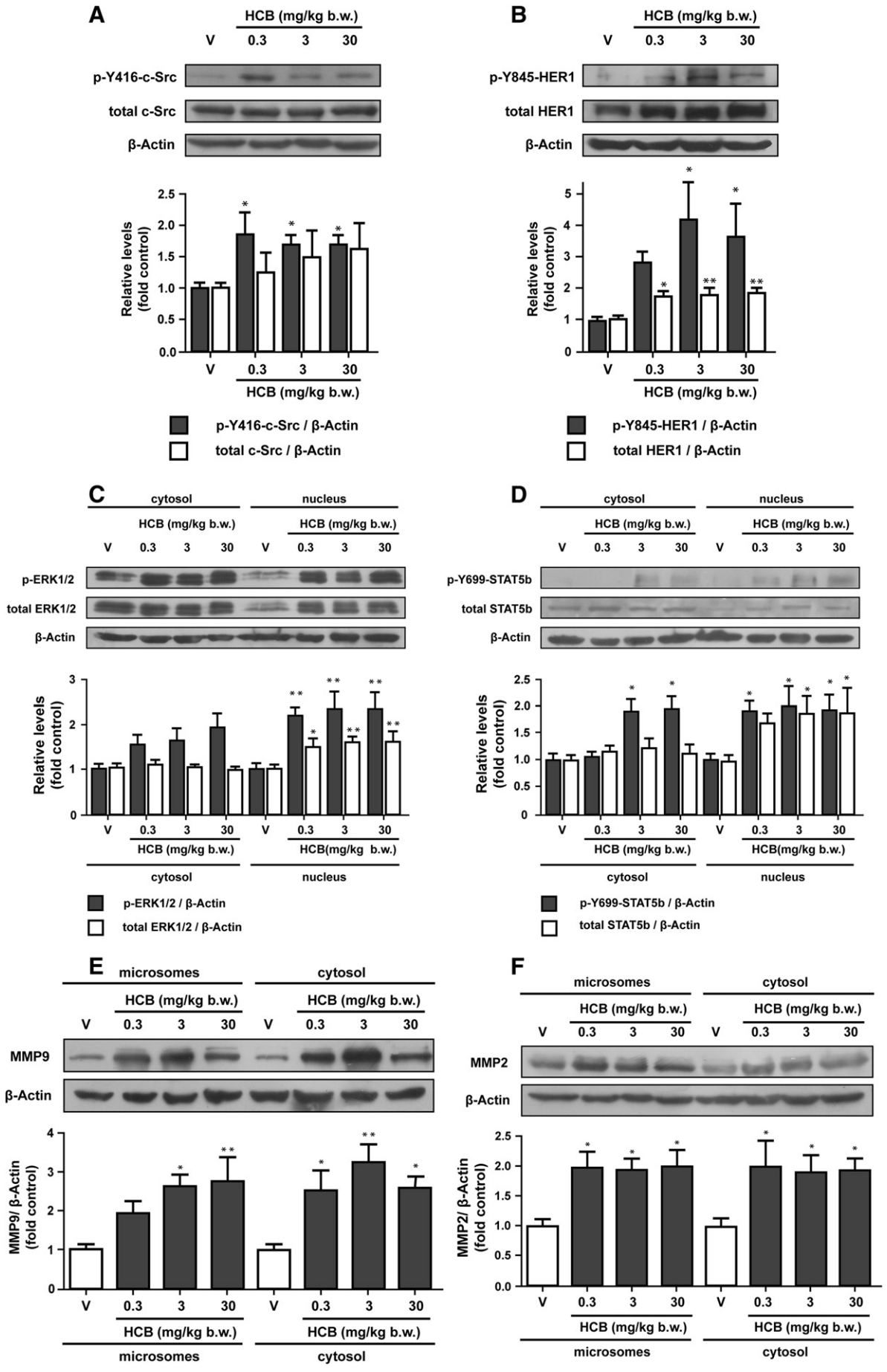
A
HCB (mg/kg b.w.)
V 0.3 3 30
p-Y416-c-Src
total c-Src
β-Actin
Relative levels (fold control)
HCB (mg/kg b.w.)
p-Y416-c-Src / β-Actin
total c-Src / β-Actin
B
HCB (mg/kg b.w.)
p-Y845-HER1
total HER1
β-Actin
Relative levels (fold control)
HCB (mg/kg b.w.)
p-Y845-HER1 / β-Actin
total HER1 / β-Actin
C
cytosol
nucleus
HCB (mg/kg b.w.)
p-ERK1/2
total ERK1/2
β-Actin
Relative levels (fold control)
HCB (mg/kg b.w.)
HCB(mg/kg b.w.)
cytosol
nucleus
p-ERK1/2 / β-Actin
total ERK1/2 / β-Actin
D
cytosol
nucleus
HCB (mg/kg b.w.)
p-Y699-STAT5b
total STAT5b
β-Actin
Relative levels (fold control)
HCB (mg/kg b.w.)
HCB(mg/kg b.w.)
cytosol
nucleus
p-Y699-STAT5b / β-Actin
total STAT5b / β-Actin
E
microsomes
cytosol
HCB (mg/kg b.w.)
MMP9
β-Actin
MMP9/ β-Actin (fold control)
HCB (mg/kg b.w.)
HCB (mg/kg b.w.)
microsomes
cytosol
F
microsomes
cytosol
HCB (mg/kg b.w.)
MMP2
β-Actin
MMP2/ β-Actin (fold control)
HCB (mg/kg b.w.)
HCB (mg/kg b.w.)
microsomes
cytosol

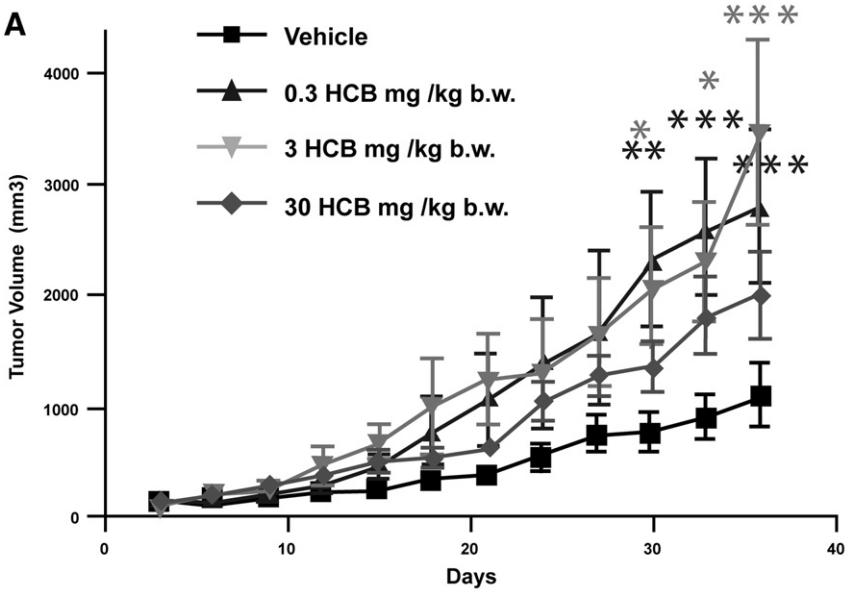

B

	Vehicle	0.3 HCBmg /kg bw	3 HCB mg/kg bw	30 HCB mg /kg bw
Tumor weight (g)	1.3 ± 0,4	4.5 ± 1,1 *	4 ± 1,1 *	3.4 ± 0,8

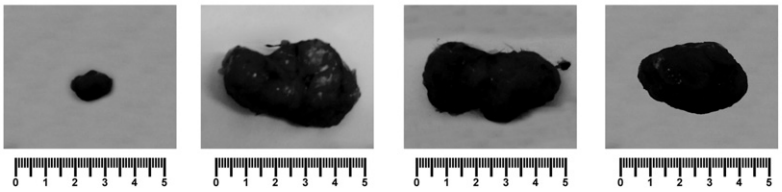

Fig. 7. HCB enhances C4-HI mammary tumor growth in BALB/c mice. (A) Tumor volume and (B) tumor weight. C4-HI tumors were transplanted s.c. into female BALB/c mice, as described in Materials and methods. After 10 days, HCB (0.3, 3, 30 mg/kg b.w.) or vehicle was administered i.p. into BALB/c mice, and tumors were measured three times a week. Animals were euthanized at 30 days after treatment and then tumors were photographed and weighed. (A) Tumor volume (mm^3) versus time (days). Statistical comparisons were made by analysis of variance (two-way ANOVA) with a 95% confidence. ANOVA: interaction, treatment factor and time factor $p < 0.0001$. ANOVA analysis was followed by Bonferroni for treatment comparisons. The values are mean ± SD of three experiments with $n = 7$ mice per group. Asterisks indicate significant differences versus vehicle ($^*p < 0.05$, $^{**}p < 0.01$, $^{***}p < 0.001$). (B) The values are mean ± SD of three independent experiments with $n = 7$ mice per group. Asterisks indicate significant differences vs. vehicle ($^*p < 0.05$), ANOVA and Tukey post hoc test.

MMP9 expression and activity, as well as cell invasion in melanoma cells. Other authors observed that AhR pathway activation enhances gastric cancer cell invasiveness likely through a c-Jun-dependent induction of MMP9 (Peng et al., 2009).

It has been demonstrated that HER1 and c-Src cooperate in breast tumor formation and progression (Biscardi et al., 1999b). Other studies found that HER1 is involved in cell invasion and metastasis in cancer (Seton-Rogers et al., 2004). In this study, we demonstrated that HCB 5 μM significantly increased MDA-MB-231 cell invasion involving c-Src, HER1, AhR and MMPs proteins. Taken together, these results suggest that HCB, after its binding to AhR, stimulates HER1/ERK1/2 signaling pathway triggering an increase of MMP9 expression, secretion and activation. In addition, HCB activates c-Src/HER1/STAT5b pathway via AhR that may be stimulating MMP2 expression. Finally, these changes in MMPs expression and activities may be involved in HCB-induced cell invasion (Fig. 5C).

Our *in vivo* studies showed that in both spontaneous tumor metastasis models (MDA-MB-231 and C4-HI), HCB (0.3 and 3 mg/kg b.w.) enhanced mammary tumor volume and weight. Concerning to metastasis analysis, we observed that HCB promotes lung metastasis in the different experimental models evaluated, regardless the hormone receptor status. In this respect, two of the models used in this study, are hormone independent (MDA-MB-231 and LM3), while the C4-HI tumor is ER and PR positive. It has been reported that organochlorine compounds exposure favors metastatic process in breast cancer. Liu et al. (2010) demonstrated that PCBs treatment of MDA-MB-231 and MCF-7 induces cell migration and increases MDA-MB-231 metastatic capacity in liver and lung *in vivo*. Eum et al. (2004) found that

Fig. 6. HCB action on Y416-c-Src and Y845-HER1 phosphorylation, ERK1/2 and STAT5b activation and MMPs protein levels in MDA-MB-231 tumors. (A) Total c-Src and phospho-Y416-c-Src, (B) total HER1 and phospho-Y845-HER1, (C) total ERK1/2 and phospho-ERK1/2, (D) total STAT5b and phospho-Y699-STAT5b, (E) MMP9 and (F) MMP2 protein levels. MDA-MB-231 cells (6×10^6) were injected into the mammary fat pad of nude mice as described in Materials and methods. Once tumors reached a volume of 50 mm^3, HCB (0.3, 3, 30 mg/kg) or vehicle was administered i.p. into mice three times a week. Animals were euthanized at 30 days after treatment and mammary tumors were used for subcellular fractionation. Microsomal, cytosol and nuclear fractions were prepared, and resolved by SDS–PAGE and blotted for p-Y416-c-Src, p-Y845-HER1, p-ERK1/2, and p-Y699-STAT5b with specific antibodies, and then reblotted for total proteins. Protein expression was relativized to β-Actin expression. Western blots from one representative experiment are shown in the upper panels. Quantification by densitometric scanning of the immunoblots is shown in the lower panels. Data are expressed as means ± SD of three independent experiments. Asterisks indicate significant differences vs. vehicle ($^*p < 0.05$, $^{**}p < 0.01$), ANOVA and Tukey post hoc test.

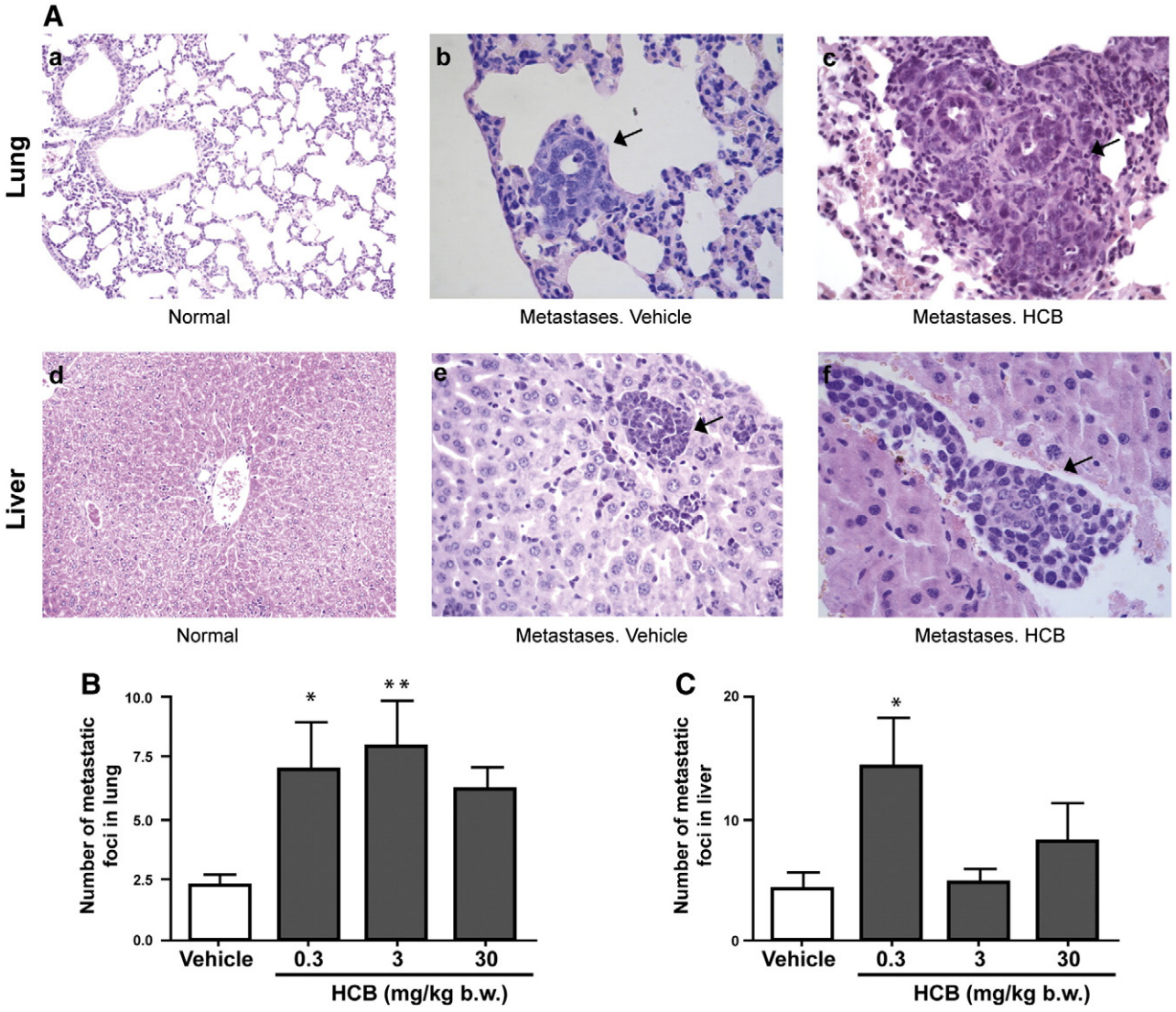

Fig. 8. HCB effect on lung and liver metastasis of C4-HI tumors. (A) Representative photomicrographs of micrometastasis: (a) normal lung and (d) normal liver (10×, HE); (b) lung or (e) liver micrometastasis of vehicle treated mice (40×, HE); (c) lung or (f) liver micrometastasis was observed after HCB-exposure (arrow) (40×, HE). (B) The number of metastatic foci per section lung, and (C) per section liver was counted. C4-HI tumors were transplanted s.c. into mice, as described in Materials and methods. After 10 days, HCB (0.3, 3, 30 mg/kg) or vehicle was administered i.p. into mice and the presence of micrometastasis in these organs was analyzed. Data are expressed as means ± SD of three independent experiments. Asterisks indicate significant differences vs. vehicle ($^{*}p < 0.05$, $^{**}p < 0.01$), ANOVA and Tukey post hoc test.

PCB104 induces MDA-MB-231 endothelial transmigration, contributing to develop breast cancer metastasis.

In the xenograft model, we found that HCB (0.3 and 3 mg/kg b.w.) enhanced mammary tumor volume and weight. Unfortunately we could not obtain enough number of metastasis in all mice to conclude about the pesticide effect in this model. On the other hand, consistent with our *in vitro* results, we observed that HCB induced an increase in c-Src/HER1/STAT5b and HER1/ERK1/2 signaling as well as MMP2 and MMP9 expression in tumors. Other authors have reported that STAT5b and ERK1/2 proteins are implicated in tumor progression (Kazansky et al., 2003; Whyte et al., 2009). Altogether, our *in vitro* and *in vivo* results with MDA-MB-231, suggest that HCB might be stimulating MMPs through the activation of these signal transduction pathways. Since it is known that MMPs play an important role in tumor growth, we hypothesize that HCB may be inducing an enhancement in tumor volume through an increase in MMPs protein levels (Fig. 5C). However, the fact that tumor growth is not enhanced in HCB (30 mg/kg b.w.) treated mice in spite of presenting an increase in MMPs expression, suggest that other mechanism may be involved, such as apoptosis. In this respect, we have previously reported that HCB induced apoptosis in MCF-7 (García et al., 2010).

In the spontaneous metastasis syngeneic model (C4-HI), we found that HCB (0.3 and 3 mg/kg b.w.) enhanced mammary tumor volume and weight. In addition, the pesticide significantly enhanced metastatic focus in lungs (HCB 0.3 and 3 mg/kg b.w.) and in liver (HCB 0.3 mg/kg b.w.), without any effect in lymphatic nodes. Considering that HCB did not alter MMPs expression in these tumors (data not shown) we cannot assume that these proteins are related with HCB-induced tumor growth. One possibility could be that HCB alters this parameter through an ER dependent mechanism. Previous results of our laboratory in MCF-7(+ERα) breast cancer cell line showed that HCB increases proliferation in an ERα-dependent manner (García et al., 2010).

Finally, in the syngeneic experimental lung metastasis LM3 model, HCB (30 mg/kg b.w.) significantly increased the number of >1.5 mm macrometastasis in lungs. The fact that HCB did not produce changes in the number of total metastasis, could be related to the higher number of metastasis obtained. The enhancement in the number of greater size metastatic foci observed in lungs, may be a consequence of HCB-induced acceleration in the invasive process, allowing the focus to be produced before, having more time for growing. Other possibilities are that the pesticide facilitates

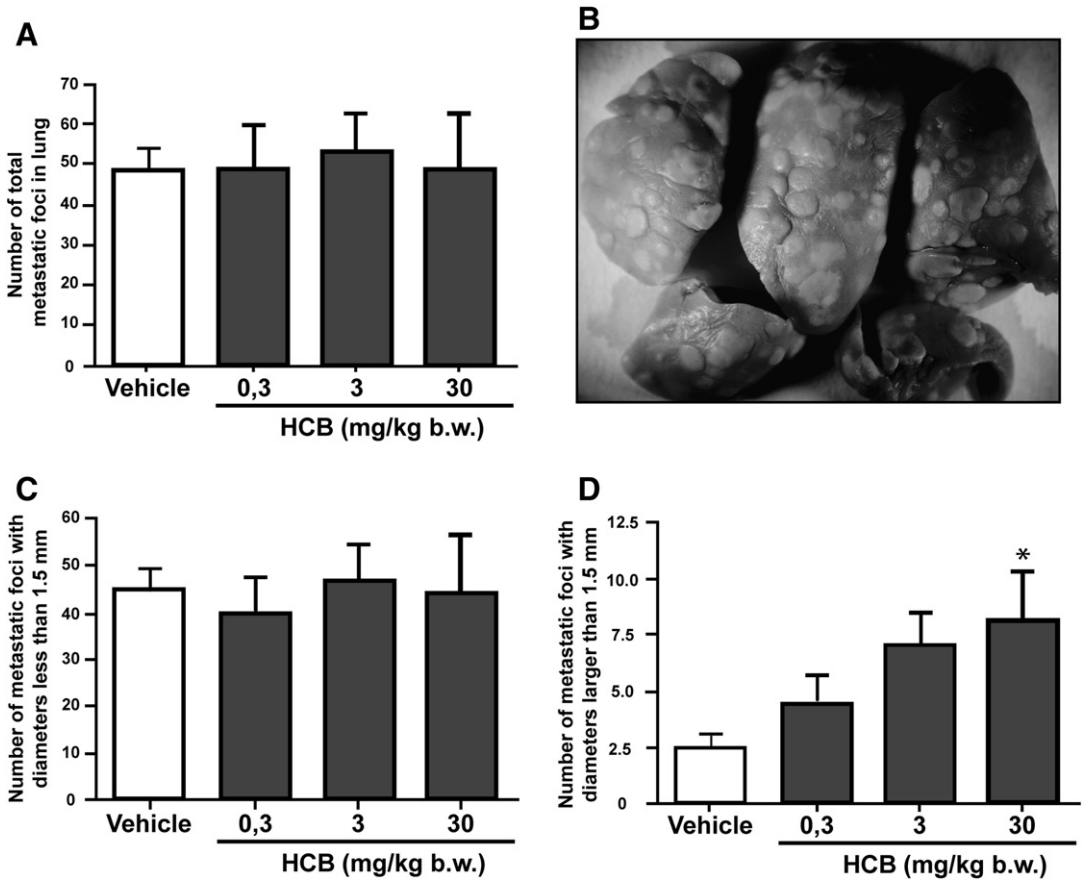

Fig. 9. HCB effect on the metastatic foci in the syngeneic experimental LM3 model. (A) Number of metastatic foci in mice lung, (B) representative photograph of mice lung with metastatic foci, (C) number of metastatic foci with diameters lower than 1.5 mm, and (D) with diameters larger than 1.5 mm. HCB (0.3, 3, 30 mg/kg) or vehicle was administered i.p. to female BALB/c mice during 2 weeks. Then, LM3 cells were i.v. inoculated into mice, and HCB treatment continued for another 3 weeks. The number and size of metastatic foci per lung were counted using stereoscopic microscope. Data are expressed as means ± SD of three independent experiments. Asterisks indicate significant differences vs. vehicle ($^*p < 0.05$), ANOVA and Tukey post hoc test.

proliferation in metastatic niches, or that some lung metastatic foci merge in a bigger one. Considering the last hypothesis, we could not discard the fact that HCB may be promoting the number of total metastatic foci.

In the present study, the highest HCB dose (5 μM) used in MDA-MB-231 cells assays *in vitro*, is in the same range of order as that found in serum from humans from a highly contaminated population (To-Figueras et al., 1997). In the *in vivo* models, mice were treated with HCB (0.3, 3 and 30 mg/kg b.w.), which were assayed previously in other toxicological studies and had an androgenic effect in mice (Ralph et al., 2003). With respect to the effective HCB doses in the different metastasis assays analyzed, HCB (0.3 and 3 mg/kg b.w.) promotes the whole metastatic process, as we found in the spontaneous metastasis model. Conversely, the HCB (30 mg/kg b.w.) may be enhancing only the last step of this process, as it has only effect in the experimental metastasis model studied.

In conclusion, we have demonstrated for the first time, that HCB induces cell invasion and MMP2 and MMP9 expression in MDA-MB-231. c-Src, HER1 pathways and AhR are involved in HCB mechanism of action. In addition, using different animal models (spontaneous and experimental metastasis), our results showed that HCB enhances tumor growth and metastasis in lung. Our findings suggest that HCB may be a risk factor for human breast cancer progression.

Funding

This research was supported by grants from National Agency of Scientific and Technological Promotion (PICT 05-25849), National Council of Scientific and Technological Research (CONICET, PIP 0739) and University of Buenos Aires (PIDs MO32 and M433).

Competing financial interest declaration

The authors declare that there are no conflicts of interest.

Acknowledgments

Paola Rojas, Claudia Cocca, Lucas Colombo, Claudia Lanari, Diana Kleiman de Pisarev and Andrea Randi are established researchers of the CONICET.

References

Agency for Toxic Substances, Disease Registry (ATSDR), 2002. Toxicological Profile for Hexachlorobenzene. U.S.D.O.H.A.H., Services, Atlanta, GA.
Alvarez, L., Hernández, S., Martínez-de-Mena, R., Kolliker-Frers, R., Obregón, M.J., Kleiman de Pisarev, D.L., 2005. The role of type I and type II 5′ deiodinases on hexachlorobenzene-induced alteration of the hormonal thyroid status. Toxicology 207, 349–362.
Biscardi, J.S., Tice, D.A., Parsons, S.J., 1999a. c-Src, receptor tyrosine kinases and human cancer. Rev. Adv. Cancer Res. 76, 61–119.
Biscardi, J.S., Maa, M.C., Tice, D.A., Cox, M.E., Leu, T.H., Parsons, S.J., 1999b. c-Src-mediated phosphorylation of the EGFR on Tyr845 and Tyr1101 is associated with modulation of receptor function. J. Biol. Chem. 274, 8335–8343.
Bradford, M.M., 1976. A rapid and sensitive method for the quantitation of microgram quantities of protein utilizing the principle of protein-dye binding. Anal. Biochem. 72, 248–254.
Catterall, J.B., Carrère, S., Koshy, P.J., Degnan, B.A., Shingleton, W.D., Brinckerhoff, C.E., Rutter, J., Cawston, T.E., Rowan, A.D., 2001. Synergistic induction of MMP-1 by interleukin-1alpha and oncostatin M in human chondrocytes involves STAT

and AP-1 transcription factors via a novel mechanism. Arthritis Rheum. 44, 2296–2310.
Chambers, A.F., Matrisian, L.M., 1997. Changing views of the role of MMPs in metastasis. J. Natl. Cancer Inst. 89, 1260–1270.
Connor, K., Ramamoorthy, K., Moore, M., Mustain, M., Chen, I., Safe, S., Zacharewski, T., Gillesby, B., Joyeux, A., Balaguer, P., 1997. Hydroxylated PCBs as estrogens and antiestrogens: structure-activity relationships. Toxicol. Appl. Pharmacol. 145, 111–123.
Dietrich, C., Kaina, B., 2010. The AhR in the regulation of cell-cell contact and tumor growth. Carcinogenesis 31, 1319–1328.
Duffy, M.J., Maguire, T.M., Hill, A., Mc Dermott, E., O'Higgins, N., 2000. Metalloproteinases: role in breast carcinogenesis, invasion and metastasis. Rev. Breast Cancer Res. 2, 252–257.
Eum, S.Y., Lee, Y.W., Henning, B., Toborek, M., 2004. VEGF regulates PCB 104-mediated stimulation of permeability and transmigration of breast cancer cells in human microvascular endothelial cells. Exp. Cell Res. 296, 231–244.
García, M.A., Peña, D., Alvarez, L., Cocca, C., Pontillo, C., Bergoc, R., Kleiman de Pisarev, D.L., Randi, A.S., 2010. Hexachlorobenzene induces cell proliferation and IGF-I signaling pathway in an estrogen receptor alpha-dependent manner in MCF-7 breast cancer cell line. Toxicol. Lett. 192, 195–205.
Hahn, M.E., Goldstein, J.A., Linko, P., Gasiewicz, T.A., 1989. Interaction of hexachlorobenzene with the receptor for 2,3,7,8-tetrachlorodibenzo-p-dioxin *in vitro* and *in vivo*. Arch. Biochem. Biophys. 270, 344–355.
Ishida, M., Mikami, S., Kikuchi, E., Kosaka, T., Miyajima, A., Nakagawa, K., Mukai, M., Okada, Y., Oya, M., 2010. Activation of the AhR pathway enhances cancer cell invasion by upregulating the MMP expression and is associated with poor prognosis in upper urinary tract urothelial cancer. Carcinogenesis 31, 287–295.
Kazansky, A.V., Spencer, D.M., Greenberg, N.M., 2003. Activation of STAT5 is required for progression of autochthonous prostate cancer: evidence from the transgenic adenocarcinoma of the mouse prostate system. Cancer Res. 63, 8757–8762.
Kloth, M.T., Laughlin, K.K., Biscardi, J.S., Boerner, J.L., Parsons, S.J., Silva, C.M., 2003. STAT5b, a mediator of synergism between c-Src and the EGFR. J. Biol. Chem. 278, 1671–1679.
Kung, T., Murphy, K.A., White, L.A., 2009. The AhR pathway as a regulatory pathway for cell adhesion and matrix metabolism. Biochem. Pharmacol. 77, 536–546.
Lanari, C., Lamb, C.A., Fabris, V.T., Helguero, L.A., Soldati, R., Bottino, M.A., Giulianelli, S., Cerliani, J.P., Wargon, V., Molinolo, A., 2009. The MPA mouse breast cancer model: evidence for a role of progesterone receptors in breast cancer. Rev. Endocr. Relat. Cancer 16, 333–350.
Lee, C.W., Lin, C.C., Lin, W.N., Liang, K.C., Luo, S.F., Wu, C.B., Wang, S.W., Yang, C.M., 2007. TNF-α induces MMP-9 expression via activation of Src/EGFR, PDGFR/PI3K/Akt cascade and promotion of NFκB/p300 binding in human tracheal smooth muscle cells. Am. J. Physiol. Lung Cell Mol. Physiol. 292, L799–L812.
Liu, S., Li, S., Du, Y., 2010. Polychlorinated biphenyls (PCBs) enhance metastatic properties of breast cancer cells by activating Rho-associated kinase (ROCK). PLoS One 5, e11272.
Luo, Y., Liang, F., Zhang, Z.Y., 2009. PRL1 promotes cell migration and invasion by increasing MMP2 and MMP9 expression through Src and ERK1/2 pathways. Biochemistry 48, 1838–1846.
Matsumura, F., 1994. How important is the protein phosphorylation pathway in the toxic expression of dioxin-type chemicals? Biochem. Pharmacol. 48, 215–224.
Meng, D., Lv, D.D., Zhuang, X., Sun, H., Fan, L., Shi, X.L., Fang, J., 2009. Benzo[a]pyrene induces expression of MMPs and cell migration and invasion of vascular smooth muscle cells. Toxicol. Lett. 184, 44–49.
Miller, M.E., Holloway, A.C., Foster, W.G., 2005. Benzo-[a]-pyrene increases invasion in MDA-MB-231 breast cancer cells via increased COX-II expression and PGE2 output. Clin. Exp. Metastasis 22, 149–156.
Mylchreest, E., Charbonneau, M., 1997. Studies on the mechanism of uroporphyrinogen decarboxylase inhibition in hexachlorobenzene-induced porphyria in the female rat. Toxicol. Appl. Pharmacol. 145, 23–33.
Park, S., Dong, B., Matsumura, F., 2007. Rapid activation of c-Src kinase by dioxin is mediated by the Cdc37-HSP90 complex as part of AhR signaling in MCF10A cells. Biochemistry 46, 899–908.
Parsons, S.J., Parsons, J.T., 2004. Src family kinases, key regulators of signal transduction. Oncogene 23, 7906–7909.
Peña, D., Pontillo, C., García, M.A., Cocca, C., Alvarez, L., Chiappini, F., Bourguignon, N., Frahm, I., Bergoc, R., Kleiman de Pisarev, D., Randi, A., 2012. Alterations in c-Src/HER1 and estrogen receptor-α signaling pathways in mammary gland and tumors of hexachlorobenzene-treated rats. Toxicology 293, 68–77.
Peng, T.L., Chen, J., Mao, W., Song, X., Chen, M.H., 2009. AhR pathway activation enhances gastric cancer cell invasiveness likely through a c-Jun-dependent induction of MMP-9. BMC Cell Biol. 10, 27–34.
Pontillo, C., García, M.A., Peña, D., Cocca, C., Chiappini, F., Alvarez, L., Kleiman de Pisarev, D., Randi, A.S., 2011. Activation of c-Src/HER1/STAT5b and HER1/ERK1/2 signaling pathways and cell migration by hexachlorobenzene in MDA-MB-231 human breast cancer cell line. Toxicol. Sci. 120, 284–296.
Ralph, J.L., Orgebin-Crist, M.C., Lareyre, J.J., Nelson, C.C., 2003. Disruption of androgen regulation in the prostate by the environmental contaminant hexachlorobenzene. Environ. Health Perspect. 111, 461–466.
Randi, A.S., Cocca, C., Carbone, V., Nuñez, M., Croci, M., Gutiérrez, A., Bergoc, R., Kleiman de Pisarev, D.L., 2006. Hexachlorobenzene is a tumor co-carcinogen and induces alterations in IGFs signaling pathway in the rat mammary gland. Toxicol. Sci. 89, 83–92.
Seton-Rogers, S.E., Lu, Y., Hines, L.M., Koundinya, M., LaBaer, J., Muthuswamy, S.K., Brugge, J.S., 2004. Cooperation of the ErbB2 receptor and TGFbeta in induction of migration and invasion in mammary epithelial cells. Proc. Natl. Acad. Sci. U. S. A. 101, 1257–1262.
Soto-Guzmán, A., Navarro-Tito, N., Castro-Sánchez, L., Martínez-Orozco, R., Pérez-Salazar, E., 2010. Oleic acid promotes MMP-9 secretion and invasion in breast cancer cells. Clin. Exp. Metastasis 27, 505–515.
To-Figueras, J., Sala, M., Otero, R., Barrot, C., Santiago-Silva, M., Rodamilans, M., Herrero, C., Grimalt, J., Sunyer, J., 1997. Metabolism of Hexachlorobenzene in humans: association between serum levels and urinary metabolites in a highly exponed population. Environ. Health Perspect. 105, 78–83.
Urtreger, A., Ladeda, V., Puricelli, L., Rivelli, A., Vidal, M., Delustig, E., Joffe, E., 1997. Modulation of fibronectin expression and proteolytic activity associated with the invasive and metastatic phenotype in two new murine mammary tumor cell lines. Int. J. Oncol. 11, 489–496.
Villano, C.M., Murphy, K.A., Akintobi, A., White, L.A., 2006. 2,3,7,8-Tetrachlorodibenzo-p-dioxin induces MMPs expression and invasion in A2058 melanoma cells. Toxicol. Appl. Pharmacol. 210, 212–224.
Wang, C., Navab, R., Iakovlev, V., Leng, Y., Zhang, J., Tsao, M.S., Siminovitch, K., Mc Cready, D.R., Done, S.J., 2007. Abelson interactor protein-1 positively regulates breast cancer cell proliferation, migration, and invasion. Mol. Cancer Res. 5, 1031–1039.
Whyte, J., Bergin, O., Bianchi, A., Mc Nally, S., Martin, F., 2009. Key signalling nodes in mammary gland development and cancer. MAP kinase signalling in experimental models of breast cancer progression and in mammary gland development. Breast Cancer Res. 11, 209–212.